EuroGeo4 Paper number 229

FULL SCALE TESTING OF GEOGRIDS TO EVALUATE JUNCTION STRENGTH REQUIREMENTS FOR REINFORCED ROADWAY BASE DESIGN

Barry Christopher[1] & Steve Perkins[2]

[1] *Christopher Consultants. (e-mail: Barryc325@aol.com)*
[2] *Montana State University. (e-mail: stevep@ce.montana.edu)*

Abstract: This paper presents the results of full scale laboratory tests on geogrid reinforcements in unpaved roadway sections following the procedures in the American Association of State and Highway Transportation Officials (AASHTO) 4E-SR. The test sections were instrumented to measure geosynthetic deformation. The primary focus of the test program was to evaluate the performance of geogrids and geocomposites in soft subgrade conditions in relation to the deformation of the roadway section (rutting) and the development of permanent strains in the geogrid during traffic loading. In addition, this study was performed to evaluate the integrity and performance requirements for geogrid junctions. Junctions are required to survive large deformations associated with rutting of the subgrade during construction. Junctions must also provide the majority of the geogrid interaction in subgrade stabilization and base reinforcement by transferring lateral stress into the tensile elements under cyclic strains. This paper provides a brief description of the test section construction procedures, equipment, materials, instrumentation and test protocol. The results of the full scale test in terms of rutting in two geogrid sections versus a no geogrid control section will be presented. A post construction evaluation of the geogrid integrity including any loss of strength will be provided. The results of the stress strain response of the geogrid measured in the full scale tests will then be compared to the junction strength and modulus using index test methods (e.g., modified GRI GG2 procedures) and performance measurements from pullout tests reported by the authors in a separate paper (Christopher et al., 2008). This comparison will be used to support junction strength requirements for geogrids used in reinforced roadway base applications.

Keywords: cyclic load, geogrid, interaction, reinforced road, stabilization, subgrade.

INTRODUCTION

In this study, full scale laboratory roadway stabilization tests were performed on unpaved roadway test sections. Test sections were constructed using a 1 m thick silt type subgrade having a CBR of 1 percent (c_u = 30 kPa, Mr ≈ 10 MPa). The aggregate layer thickness was 300 mm. The test sections were constructed with two geosynthetics, a geogrid and a geogrid/geotextile geocomposite, as well as a control section with no geocomposite. Each section was cyclically loaded with a 300 mm plate to a peak load value of 40 kN, to mimic dynamic wheel loads. The purpose of the study was to evaluate the reinforcement benefit of these two different geosynthetic types and to determine the characteristics that contributed to the performance of the geosynthetics used in this type of soil condition. A specific geogrid characteristic of interest was the junction integrity in relation to construction survivability and reinforcement performance. Performance was defined in terms of the number of load cycles to reach a specific permanent rut depth of 76 mm in the aggregate surface layer for each test section and Traffic Benefit Ratio (TBR), which is the number of load cycles for a reinforced section divided by the number of control test load cycles to reach this same rut depth for a comparable unreinforced test section. The test sections were instrumented to measure geosynthetic deformation and subgrade pore water pressure response. The instrumentation measurements were used in the evaluation of each test section to identify the mechanical characteristics that contributed to the performance of the geosynthetic. In addition, post construction evaluation included measurement of the permanent deformation (rut) bowl at the surface as compared to the deformation at the base/subgrade interface. Junctions were also evaluated at this stage with respect to total deformation and survivability.

STABILIZATION TESTING PROGRAM

The Geotesting Express pavement test box facility was used to create the test sections presented in this report. The pavement test box facility was designed and constructed for the purpose of conducting full-scale laboratory experiments on reinforced and unreinforced pavement sections and it meets the requirements of specifications developed for AASHTO Subcommittee 4E as contained in Berg et al. (2000). The test box facility is designed to mimic pavement layer materials, geometry and loading conditions encountered in the field as realistically as possible with an indoor, laboratory based facility (Perkins, 1999, 2002). This type of test box facility allows a high degree of control to be exercised on the construction and control of pavement layer material properties.

Each roadway test section was constructed with a nominal cross-section consisting of 300 mm of base course aggregate and 1 m of subgrade soil with a CBR = 1%. The geosynthetic was placed between the base course and subgrade layers. A control test section performed on the same soil conditions and cross section without a geosynthetic was used for comparison to the geosynthetic stabilized sections. Descriptions of these components of the facility are provided in the sections below along with a description of test section construction techniques and quality control measures.

Test-Box and Loading Apparatus

Test sections were constructed in a 2 m by 2 m by 1.5 m box shown in Figure 1. The side and back walls of the box consist of 150 mm thick reinforced concrete. The front wall consists of steel channels that are removable in order to facilitate excavation of the test sections. Steel I-beams set into two of the concrete walls serve as a base for the steel I-beam loading frame. A load actuator is mounted on the load frame and consists of a pneumatic cylinder with a 300 mm diameter bore and a stroke of 75 mm. A 50 mm diameter steel rod extends from the piston of the actuator. The rod is rounded at its tip and fits into a cup welded on top of the load plate that rests on the pavement surface. The load plate consists of a 300 mm diameter steel plate with a thickness of 25 mm. A 6 mm thick, waffled butyl-rubber pad is placed beneath the load plate in order to provide uniform pressure and avoid stress concentrations along the plate's perimeter (i.e., similar to a tire load). Figure 1 shows an actual image of the test-box facility and Figure 2 shows a picture of the load plate resting on the base course surface.

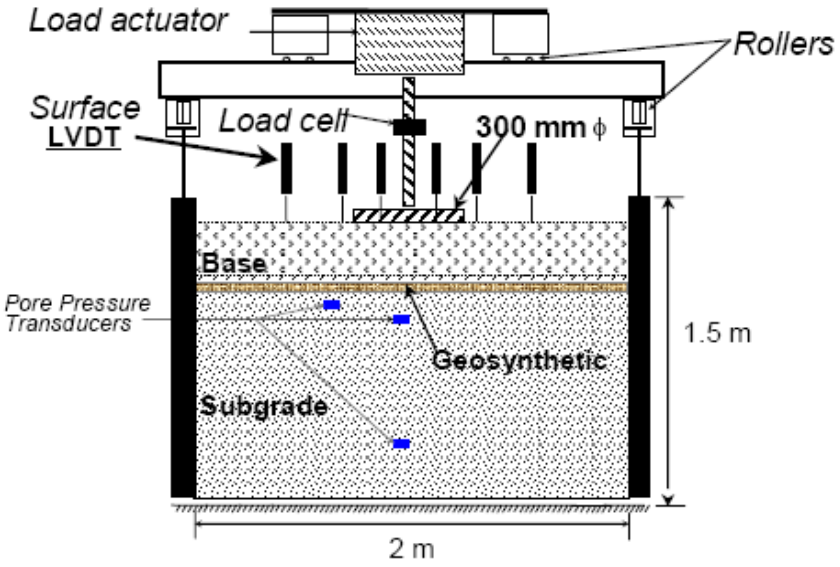

Figure 1. Schematic diagram of the pavement test facility.

Figure 2. Laboratory test setup for full scale stabilization study

A binary solenoid regulator attached to a computer controls the load-time history applied to the plate. The software is set up to provide a linear load increase from zero to 40 kN over a 0.3 second rise time, followed by a 0.2 second period where the load is held constant, followed by a load decrease to zero over a 0.3 second period and finally followed by a 0.5 second period of zero load before the load cycle is repeated, resulting in a load pulse frequency of 0.67 Hz. The maximum applied load of 40 kN results in a pressure on the base course of 550 kPa, which could also be considered equivalent to a tire pressure. This load represents one-half of an axle load from an equivalent single axle load (ESAL). In test sections where significant deformation (more than 25 mm) occurred during the initial applied load cycles, the full load could not be maintained (with a measured drop off of up to 20%). Thus, periodic adjustments

were required during the tests. In order to provide a uniform basis of comparison of the results, the number of cycles was corrected to an equivalent load of 40 kN using a fourth order polynomial equation (i.e., the same as used for traffic simulation in the design of roadway sections).

Instrumentation

Instrumentation was used in each test section to evaluate rutting in the stabilization aggregate, strain distribution in the reinforcement with distance away from the wheel load, and pore water pressure response of the subgrade during placement, compaction and subsequent loading. Instrumentation was included to make the following measurements:

- Vertical surface deformation in the stabilization aggregate layer using 100 mm RDP Group Type DCT linear voltage displacement transducers (LVDT's) as shown in Figure 1 and 2.
- Applied load to the plate using a calibrated load cell (see Figure 1).
- Pore pressure in the subgrade during construction and pavement loading using low air entry porous stones connected to Sensym Model No. V0030G2A pore pressure transducers.
- The geosynthetics were instrumented with wire extensometers as shown in Figure 3, which were connected to LVDTs to measure the transfer of stress away from the wheel loading area (a basic input parameter for mechanistic-empirical design). Bonded resistance strain gauges were also mounted on geogrid ribs between wire gages for redundancy in strain measurements.
- Measurements were made on the geosynthetics at the front of the test box using a 0.5 mm scale to determine if any movement was occurring at the edge of the box during application of load.

A) 

B) 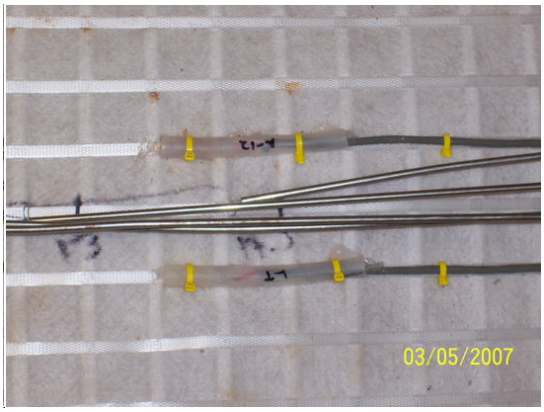

Figure 3. Wire extensometers and bonded resistance gages mounted geogrid/geotextile geocomposite showing a) position on geosynthetic and b) close-up of gages.

Geosynthetic Materials

Two geosynthetics were used in this study: 1) a welded polypropylene biaxial geogrid ($GG_{wd\text{-}pp}$), and 2) a geogrid/geotextile geocomposite ($GC_{gg\text{-}nwgt}$) consisting of a welded polypropylene biaxial geogrid with a 151 g/m^2 polypropylene needle punched nonwoven geotextile firmly bonded between the cross laid reinforcement ribs. The relevant properties of these two materials are shown in Table 1.

Table 1. Geosynthetic characteristics based on manufacturer's literature

Property	**Geosynthetic**	
	$GG_{wd\text{-}pp}$	**$GC_{gg\text{-}nwgt}$**
T_{ult} MD/XD (kN/m)	24 / 24	30 / 30
$T_{2\%}$ MD/XC (kN/m)	8 / 8	13 / 13
$T_{junction}$*MD/XD (kN/m)	9.3 / 9.4	NA ‡
$T_{2\%\text{-}junction}$† MD/XD (kN/m)	7.9 / 7.8	NA ‡

* Junction Strength measured using Geosynthetic Research Institute GRI-GG2 Method B.
† Junction Modulus from Christopher et al., 2008.
‡ Not Applicable

Subgrade Soil

Piedmont silt from Georgia was used for the subgrade. This residual soil was selected based on its problematic construction characteristics that include pumping and weaving at near optimum moisture contents, which usually requires chemical or mechanical stabilization, especially when wet of optimum (as is most often the case). Residual soils tend to retain the parent rock structure (e.g., joints and fractures) with additional fractures occurring due to stress relief during excavation. Excess water collected in this structure results in a high sensitivity when disturbed. Mica is often contained in these soils and acts somewhat like a lubricant. These soils are typically found in and around the Piedmont geophysical region of South-eastern United States as well as many other regions. These soils are also characterized by a relatively fast dissipation of pore water pressure as opposed to more cohesive soils, which was also a consideration in their selection. The soil was provided by Georgia Department of Transportation. Gradation tests (ASTM 422 and ASTM 1140) indicated that the soil was a micaceous sandy silt (ML-MH) with 95 % passing a 1 mm sieve and 55% passing a 0.075 mm sieve. The soil was found to have a maximum dry unit weight of about 15 kN/m^3 at an optimum moisture content of 22% based on standard Proctor moisture density tests (ASTM D 698); however, the soil had a natural moisture content of over 40% as delivered to the laboratory.

Base Course Aggregate

The base course material used in all test sections was a graded aggregate base meeting Georgia Department of Transportation specifications. Standard Proctor compaction test (ASTM D 698) and gradation tests were performed on the aggregate base course. The aggregate has a maximum dry unit weight of 22.7 kN/m^3 at an optimum moisture content of 5.4%. The gradation results indicated that the aggregate was a well graded gravel with 100% smaller than 20 mm and 8% finer than 0.075 mm. The graded aggregate base was estimated to have a friction angle of 43° based on large direct shear tests that had been previously performed on similar materials by the laboratory performing the tests.

Test Setup and Procedures

The silt type subgrade material was placed at a moisture content of approximately 35% to produce a CBR value of approximately 1% (the common saturated CBR value for this material in the field) under the applied compaction effort. The subgrade was constructed in approximately eight, 150 mm lifts and compacted with a gasoline powered "jumping jack" trench compactor. An extensive quality control program was performed during placement to provide consistent conditions between test sections. Moisture content and strength test were performed at a number of locations on each lift. Density tests were periodically performed using a nuclear gage calibrated against tube samples. Each lift was surveyed with a standard auto level at five locations to confirm its thickness.

The CBR was controlled during placement in the test sections using both moisture content and a hand held Pilcon vane shear strength. Laboratory tests indicated that a vane shear strength of 30 kPa correlated directly to a CBR = 1% for the silt type soil. Based on experience with previous test sections, after placement of a subgrade layer, vane shear strengths were taken on the preceding layer and required to be 5 % below target value to allow for some strengthening due to consolidation and confinement. If the target value was exceeded (e.g., due to construction delays), then the upper 600 mm of subgrade were excavated, rewetted and replaced.

The final subgrade surface was surveyed and the reinforcement was placed directly on top of the subgrade layer. One edge of the geosynthetic reinforcement was extended through a slot in the test-box face in order to measure any movement of the geosynthetic at the edge of the box during testing.

The base course material was mixed with the fork lift loader to a target water content of approximately 6 % and placed in two 150-mm lifts for a total thickness of 300 mm. The subgrade surface and the final surface of the base were surveyed to confirm the thickness. Compaction was achieved with an 8-hp vibratory plate compactor. Density measurements taken with a nuclear densometer indicated an average dry density of 21.4 kN/m^3 with a coefficient of variation of 2.3%.

The aggregate layer thickness was designed to result in 76 to 100 mm of rutting under moderate traffic (1000 cycles) based on the procedures in the FHWA Geosynthetics Design and Construction Guidelines (Holtz et al., 1998). The FHWA charts indicated that a 300 mm base course layer is required to limit the rut depth to 76 – 100 mm for moderate traffic (~1000 cycles) of an 80 kN axle load for a CBR = 1% subgrade.

A 40 kN initial load was applied to a 300 mm diameter plate resting on the surface of the aggregate base. A waffled rubber pad was placed beneath the load plate to provide a uniform load over the gravel surface. The load was cycled on the plate at a period of approximately 1.5 seconds. Load cycles were applied until a permanent surface deformation below the plate of at least 76 mm was reached or a minimum of 10,000 cycles, whichever occurred first. After the required rutting had occurred, in most cases the rut was filled in with aggregate (i.e., brought back to the original grade) and the test was repeated. These tests allow the evaluation of this recommended and common practice used in roadway stabilization applications, which also induce additional deformation on the geogrid.

STABILIZATION TEST RESULTS

The primary results of the stabilization tests are in terms of the deformation response of the aggregate layer. As indicated in the Stabilization Testing Program – Test Setup and Procedures section, the number of cycles was adjusted to provide an equivalent performance under a 40 kN load using an equivalent load factor from a 4th order polynomial equation, similar to that used for traffic simulation, as shown in Equation 1

$$\text{Load Factor} = (\text{Actual Load} / \text{Target Load})^4 \quad [1]$$

The load factor was applied to each recorded cycle with the cumulative load cycles used in the plots. This does not affect the magnitude of deformation or the shape of the curve, but shifts the curve by reducing the number of cycles for a given deformation to account for load reductions that occurred during several of the tests.

Figure 4 provides a summary of the permanent deformation response over the first 1,000 load cycles for all test sections constructed with 300 mm of aggregate and a CBR = 1%. Figure 5 presents the corresponding deformation response measured on the geogrid. A summary of the deformation response Table 3 provides a comparison of the performance characteristics from each test section, including the number of cycles and the corresponding Traffic Benefit Ratio (TBR) for each of the test results at 1 inch and 3 in. (76 mm) of rutting. Also shown is the maximum strain measured in the geosynthetic (where possible) and the rut bowl dimensions at the end of these tests. Finally Figure 6 shows the pore pressure response measured in the subgrade during cyclic loading.

Post test results included a measure of the deformation bowl at the surface of the base course and at the base course/subgrade interface as shown in the photos in Figure 7 and Figure 8 for the measured results shown in Table 3.

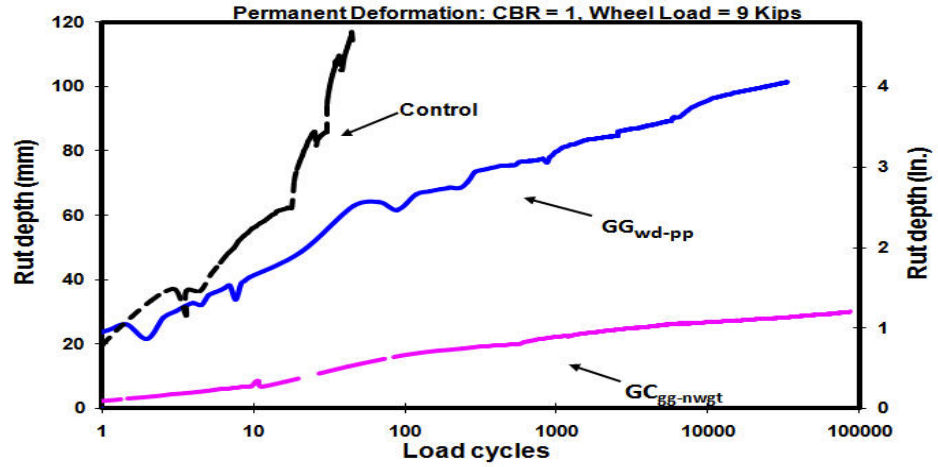

A)

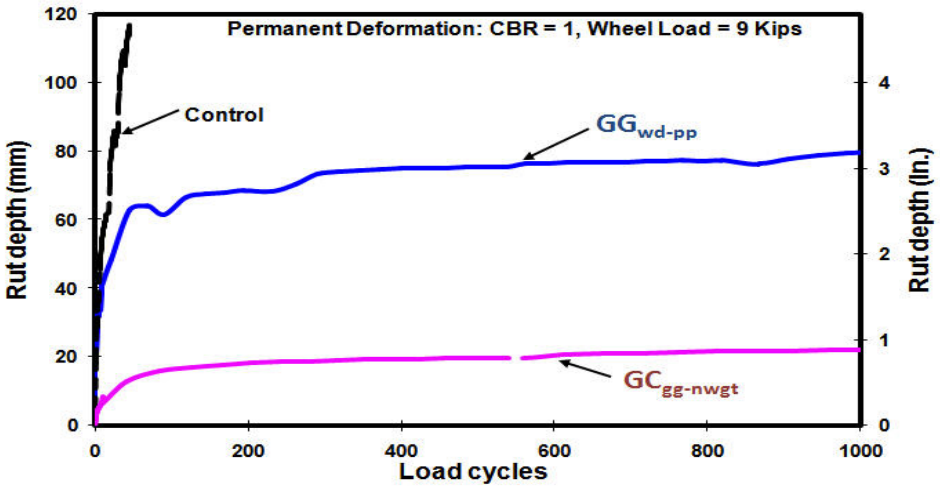

B)

Figure 4. Permanent deformation response versus load cycles for a) 100,000 and b) 1000 cycles.

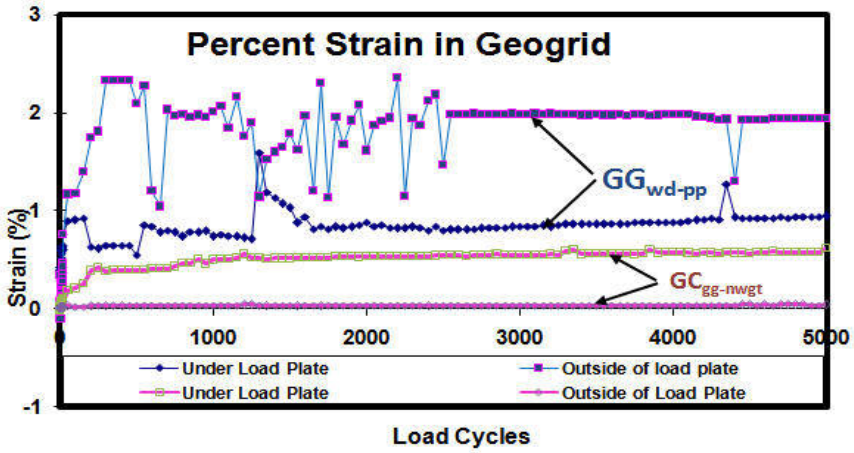

Figure 5. Geogrid strain measurements from wire extensometers mounted on $GC_{gg\text{-}nwgt}$

Table 3. Performance characteristics of each test section

Section	Number of Cycles		TBR		Maximum Measured Strain in Geosynthetic (%)	Subgrade Permanent Deformation Bowl at end of test***	
	25-mm rut	75-mm rut	25-mm rut	75-mm rut		Diameter (mm)	Depth (mm)
Control*	1.5	20	1	1	--	760	100
GG_{wd-pp}	2	540	1.3	27	2.3†	1100	43
$GC_{gg-nwgt}$	3400	>100,000	2270	>5000	‡	Bowl not apparent	Bowl not apparent

* Average of two tests
† Extensometers
‡ Strain gage – gage failure
*** Note: Bowl measurements include deformations after filling in the initial rut.

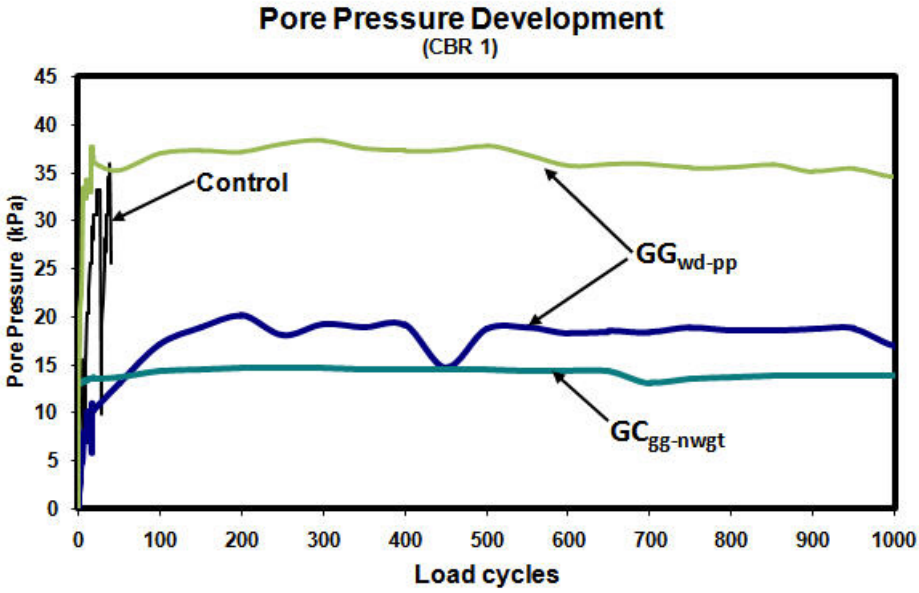

Figure 6. Pore pressure in subgrade versus number of cycle loads.

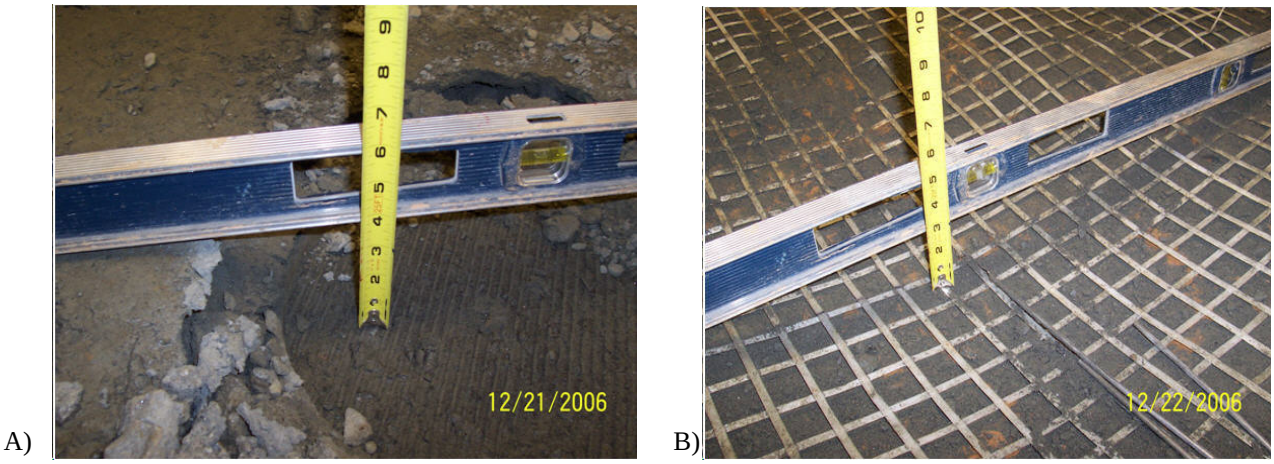

Figure 7. GG_{wd-pp} photos after testing showing the deformation (rut) at a) the base course surface and b) the geogrid subgrade interface.

A) 

B) 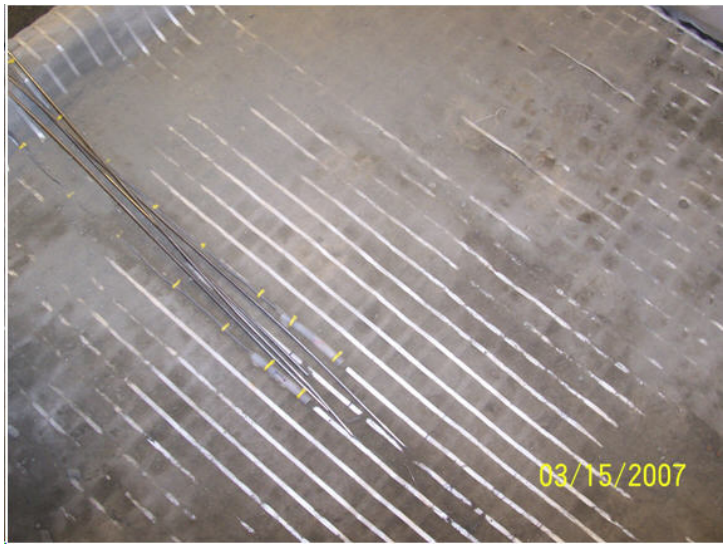

Figure 8. $GC_{gg\text{-}nwgt}$ photos after testing showing the deformation (rut) at a) the base course surface and b) the geogrid subgrade interface (no apparent rut bowl).

DISCUSSION OF RESULTS

The results from Figure 4 and Table 3 clearly show a difference in the performance of the geosynthetics evaluated in this study with $GC_{gg\text{-}nwgt}$, the geogrid/nonwoven geocomposite, performing the best. The geocomposite test was terminated at 100,000 cycles of loading at a maximum permanent rut depth of 30 mm. $GG_{wd\text{-}pp}$, the open geogrid may be at a disadvantage with the silt type soil. The soil can easily be penetrated by gravel particles and thus some of the deformation may be the result of aggregate penetration until interlock is developed. Also, the gradation of the gravel does not meet standard filter/separator criteria for the silt (e.g., the D_{15} of the gravel {i.e., 0.5 mm} is greater than 5 times the D_{15} of the subgrade {i.e., 0.02 mm}; Bertram, 1940). Regardless, the geogrid provided the anticipated deformation response based on the original design model (i.e., 76 to 100 mm of rutting in 1000 cycles as shown in Figure 4).

The surprise is the geocomposite, which incurred only 25 mm of rutting in 2270 cycles and did not approach the anticipated design value in 100,000 cycles (see Figure 4). The pore pressure data in Figure 6 provides an explanation for the difference in performance of these two geosynthetics. The pore pressure directly corresponds to the results in Figure 4 with high initial pore pressure developing for Control and $GC_{gg\text{-}nwgt}$ test sections where the largest amount of deformation per cycle was measured. These results also indicate that disturbance in the control section and aggregate penetration in the open geogrid section leads to high pore water pressure and thus a reduction in subgrade strength and correspondingly increased rutting. The increase in pore water pressure reduces the effective strength of the soil. Recent work by the authors (in a separate paper at this conference) have found good predictions of performance can be achieved by using mechanistic methods and appropriately adjusting the shear strength and modulus of the subgrade due to the excess pore water pressure.

With regards to the deformation response of the geogrid ($GG_{wd\text{-}pp}$) and corresponding strain, the maximum strain of 2.3% corresponds very well to that observed in previous tests by the authors (Christopher et al., 2008). Figure 7 shows that the geogrid ribs and junctions survived the cyclic loading under that strain and a corresponding maximum deformation of 100 mm. Wide width tests on geogrid specimens taken inside the rut bowl after the stabilization test showed no loss in strength and an apparent increase in modulus ($T_{2\%\ after\ test}$ = 20 kN/m), most likely due to strain hardening. Some minor damage was observed on the lower strength geogrid in a few junctions outside of the bowl, including partial delamination of some junctions (observed along five ribs) and failure of straps at two locations, some of which may have occurred during excavation. It should also be noted that the 2.3 % strain in the geogrid occurred just outside the load plate within the rut bowl. No junction failures occurred within the bowl, even though the ultimate junction strength is only slightly greater than the strength of the geogrid at 2% strain. Again, the geogrid performed as intended, therefore these junction issues are considered minor. This data supports the use of a geogrid design strength at 2% strain (i.e., the 2% secant modulus of the geogrid) as identified by Berg et al., 2000 and proposed by Kupec et al., 2004. A junction strength at 2% strain as proposed by Christopher et al., 2008 would also appear to be an appropriate design value.

No rib damage or junction failures were observed on the geocomposite ($GC_{gg\text{-}nwgt}$), as can be seen in Figure 8. This is not surprising considering that only 20 mm of total deformation occurred and that the strain in the grid was on the order of 0.5%.

CONCLUSIONS

This paper has presented results of full scale laboratory tests on geogrid and geocomposite (geogrid and geotextile) reinforced unpaved roadway sections. A control section containing no reinforcement shows a rapid increase in rutting with applied cyclic pavement load, reaching 75 mm of rut depth in 20 load cycles. Measurements of pore water pressure in the subgrade indicate a correspondingly rapid increase in pore water pressure, reaching a value of 35 kPa by the end of the test. A test section with an open geogrid shows a marked improvement in rutting behaviour, where the initial rapid increase in rutting stabilizes before 75 mm of rut depth is reached such that 540 load cycles can be applied before reaching 75 mm of rut. Measurements of pore water pressure mirror this result by showing the pore pressure to stabilize at a value of over 35 kPa during loading and approximately 20 kPa during unloading. The section with the geocomposite shows the best performance both in terms of rutting and pore water pressure development. In this section, 100,000 load cycles were applied while a rut depth of approximately 30 mm was seen. Pore water pressure developed rapidly but stabilized at a value of approximately 12 kPa during both loading and unloading.

These results indicate that the development of pore water pressure in the subgrade is largely responsible for the rutting seen in the roadway. In simple terms, techniques that can limit the development of excess pore water pressure in the subgrade will result in lower levels of rutting. The use of geosynthetics for stabilization has been shown to be a technique that limits excess pore water pressure development. The reinforcement action of an open geogrid positively results in such an action. The addition of a nonwoven geotextile to the reinforcement geogrid provides additional separation and filtration features that further limit the development of excess pore water pressure and further reduces rutting.

Evaluation of the geosynthetics after construction found little to no damage. The integrity of the geocomposite was unimpaired. Some minor junction damage was observed on the weaker, open geogrid, which was subjected to a vertical deformation of over 100 mm and a corresponding measured strain in the geogrid of 2.3%. No strength loss was observed and the geogrid performed as anticipated based on the original design. The strength of the geogrid and junctions at 2% strain appears to be an appropriate value for design in base and subgrade reinforcement applications.

Acknowledgements: The authors would like to acknowledge the financial support of NAUE GmbH & Co. KG for the performance of this study, Geotesting Express for their performance of the testing program, Geocomp Corporation for their contribution to the instrumentation of the test section, and the Georgia Department of Transportation for providing the soil used in this study. Special thanks go to Dr. Allen Marr for his significant input in the interpretation of the data and Mr. Jianren Wang and Mr. Marty Molino for their oversight and technical contributions during the testing program.

Corresponding author: Dr. Barry Christopher, Christopher Consultants, 210 Boxelder Lane, Roswell, GA, 30076, United States of America. Tel: 1 770 641 8696. Email: barryc325@aol.com.

REFERENCES

AASHTO. 1993. AASHTO Guide for Design of Pavement Structures, American Association of State Highway and Transportation Officials, Washington, D.C.

ASTM. 2006. Geosynthetics, Annual Books of ASTM Standards, Volume 4.13, American International, West Conshohocken, PA.

ASTM. 2007. Soil and Rock, Annual Books of ASTM Standards, Volumes 4.08 and 4.09, American International, West Conshohocken, PA.

Berg, R.B., Christopher, B. R. and Perkins, S. 2000.. Geosynthetic Reinforcement of the Aggregate Base/Subbase Courses of Pavement Structures, prepared for American Association of Highway and Transportation Officials Committee 4E, Prepared by the Geosynthetic Materials Association, 2000, 176 p.

Bender, D.A. and Barenberg. E.J. 1978. Design and behavior of soil-fabric-aggregate systems, Transportation Research Record 671, Transportation Research Board, Washington, D.C., pp. 64-75.

Bertram, G.E. 1940. An Experimental Investigation of Protective Filters, Publications of the Graduate School of Engineering, Harvard University, No. 267, January, 1940.

Christopher, B.R., Cuelho, E.V. and Perkins, S.W. 2008. Development of Geogrid Junction Strength Requirements for Reinforced Roadway Base Design. Proceedings of GeoAmericas 2008, Cancun, Mexico (in publication).

Holtz, R.D., Christopher, B.R. and Berg, R.R. 1998. Geosynthetic Design and Construction Guidelines, U.S. Department of Transportation, Federal Highway Administration, Washington DC, Report No. HI-95-038, 1995 (revised 1998 and 2008), 396 p.

Perkins, S.W. 1999. Geosynthetic Reinforcement of Flexible Pavements: Laboratory Based Pavement Test Sections, Montana Department of Transportation, Helena, Montana, Report No. FHWA/MT-99/8106-1, 140 p.

Perkins, S.W. 2002. Evaluation of Geosynthetic Reinforced Flexible Pavement Systems Using Two Pavement Test Facilities, U.S. Department of Transportation, Federal Highway Administration, Washington, DC, Report No. FHWA/MT-02-008/20040, 120 p.